2018

Numerical Modeling of Fin-and-Tube Condenser with Wet-wall Desuperheating

Hongtao Qiao
Mitsubishi Electric Research Laboratories, United States of America, qiao@merl.com

Christopher Laughman
laughman@merl.com

Numerical Modeling of Fin-and-Tube Condenser with Wet-wall Desuperheating

Hongtao QIAO*, Christopher R. LAUGHMAN

Mitsubishi Electric Research Laboratories
Cambridge, MA 02139
{qiao, laughman}@merl.com

ABSTRACT

Current heat exchanger simulation models typically divide the condenser into three regimes (desuperheating, two-phase and subcooled) and assume that condensation does not start until the bulk refrigerant flow reaches a state of saturated vapor. However, plenty of experiments have verified that condensation can occur much earlier than that when the tube wall surface temperature drops below the dew point of refrigerant even though the bulk flow is still superheated. This phenomenon is called wet-wall desuperheating (also referred to as wet-desuperheating, or condensation from desuperheated vapor in some publications). Wet-wall desuperheating is rarely modelled in the extant heat exchanger simulations due to lack of understanding in its physical process. However, neglecting this important phenomenon may lead to substantial performance prediction errors. This paper proposes a new fin-and-tube condenser heat exchanger model to bridge the research gap. In the proposed model, the heat exchanger is divided into four regimes: dry-wall desuperheating, wet-wall desuperheating, two-phase condensation and subcooled. The existence of dry-wall desuperheating and the onset point of wet-wall desuperheating are determined by rigorous algorithms. Boundaries between different flow regimes are captured to eliminate numerical discontinuities. A tube-by-tube analysis is adopted to allow for the simulation of complex tube circuitries. Simulation studies are performed to demonstrate the capabilities of the proposed model. The results show that wet-wall desuperheating always exists in the condenser with refrigerant vapor entering at the inlet, and neglecting the phenomenon can lead to significant prediction errors for heat exchanger performance.

Keywords: Wet-wall desuperheating, Dry-wall desuperheating, Condensation, Numerical modeling, Simulation, Heat exchangers

1. INTRODUCTION

Fin-and-tube heat exchangers are widely used to transfer heat between air and working fluids in refrigeration, comfort cooling and heating applications, and play a dominant role in the performance of HVAC&R equipment. Design and optimization of fin-and-tube heat exchangers is extremely challenging due to a large number of design variables, complex manufacturing constraints and multiple conflicting objectives. Compared to the time-consuming experimental trial and error, computer-based modeling approach can shorten development cycle and acquire highly efficient designs at minimum costs. Undoubtedly, efficacy of model-based approach heavily relies on the performance prediction accuracy of heat exchanger simulation models, which should capture the major heat transfer and fluid flow characteristics of heat exchangers with high fidelity and reasonable computational complexity.

Superheated refrigerant vapor entering a condenser may pass through as many as four different flow regimes: dry-wall desuperheating, wet-wall desuperheating (also referred to as wet-desuperheating, or condensation from desuperheated vapor in some publications), two-phase condensation and subcooled (Thome, 2004), as shown in Fig. 1. The dry-wall desuperheating regime often exists near the condenser inlet where the refrigerant is superheated vapor and the heat transfer surface is at a temperature above the dew point of the refrigerant. In this regime, a portion of superheat in the refrigerant is removed through sensible/convective heat transfer along the tube. Once the tube wall surface temperature drops below the dew point of the refrigerant, a very thin film of liquid condensate can form on the wall even though the bulk flow is still superheated. From that point on, vapor is in direct contact with condensate and desuperheating of the bulk flow is accomplished by heat rejection from superheated vapor to subcooled condensate. This regime is called the wet-wall desuperheating, since the tube walls are covered by the liquid condensate. The two-phase regime starts when the bulk flow completely loses its superheat, and continues until all the saturated vapor changes into liquid. In the subcooled regime, further heat rejection from all-liquid flow cools the refrigerant to a temperature below its bubble point.

Depending upon the operating condition, dry-wall desuperheating may or may not exist in a condenser. However, wet-wall desuperheating always exists in a condenser with superheated vapor entering at the inlet. The wet-wall desuperheating phenomenon was known as early as in 1950s and its heat transfer characteristics have been experimentally investigated since then. Recently a series of noteworthy publications by Prof. Hrnjak at the University of Illinois and his collaborators experimentally verified the presence of wet-wall desuperheating (Meyer and Hrnjak, 2017). Meanwhile, their studies showed that the heat transfer coefficient (HTC) during wet-wall desuperheating increased rapidly as the bulk vapor flow gradually lost superheat, and was significantly higher than the prediction by the single-phase correlations (Kondou and Hrnjak, 2012). Accordingly, they proposed a correlation for the HTC during wet-wall desuperheating, which linearly interpolated between the two-phase and single-phase HTC correlations based on the temperature differences among the bulk vapor flow, refrigerant dew point and tube wall surface. The proposed correlation eliminated the discontinuity between the single-phase and two-phase HTC correlations at x = 1. Meanwhile, these researchers also found that the pressure drop (DP) increased during wet-wall desuperheating and deviated from the single-phase DP correlations due to the energy dissipation as a result of the presence of liquid film (Meyer and Hrnjak, 2014).

Although it has been widely accepted and acknowledged, the wet-wall desuperheating phenomenon has been rarely modelled in the heat exchanger simulations due to lack of full understanding in its underlying physics. The extant heat exchanger models generally assume that the entire desuperheating region is dry and condensation does not take place until the bulk flow becomes saturated vapor (Domanski and Didion, 1983; Lee and Domanski, 1997; Liang *et al.*, 2001; Liu *et al.*, 2004; Jiang *et al.*, 2006). This simplifying assumption can significantly reduce modeling complexity, but it could substantially oversize heat exchangers. On the other hand, dry-wall desuperheating may not exist at all if refrigerant vapor enters the condenser with modest superheat and the tube wall temperature is lower than the dew point of the refrigerant at the inlet. Therefore, it is necessary to develop new modeling approaches to distinguish dry-wall from wet-wall desuperheating and compute the heat transfer of each flow regime separately.

Different from determining the boundary between single-phase and two-phase, seeking the boundary between dry-wall and wet-wall involves iteration of the heat transfer surface temperature. The algorithm to determine the existence of dry-wall desuperheating needs to be delicately devised, otherwise successive calculation domains, i.e., two adjacent tubes/segments along the refrigerant flow direction, could end up contradicting from each other between dry-wall and wet-wall calculations, since dry-wall desuperheating can mathematically take place after wet-wall desuperheating, but is physically impossible.

To address the above challenges, this paper proposes a new fin-and-tube condenser model that will capture the heat transfer characteristics during the desuperheating of vapor, i.e., dry-wall and wet-wall. A rigorous tube-by-tube approach is adopted for an accurate performance evaluation of heat exchanger, i.e., the performance of each tube is analyzed separately and each tube is associated with different refrigerant parameters and air mass flow rate, inlet temperature and humidity. Meanwhile, this approach allows for the analysis of complex tube circuitries and air flow propagation as well as air/refrigerant flow maldistribution. It is worthwhile to mention that the condensing subcooled regime is not analyzed in the proposed model, because there is lack of heat transfer correlations for this flow regime and usually neglecting this flow regime results in negligible errors in heat exchanger performance prediction. The remainder of the paper is organized as follows. Section 2 describes the details for the proposed heat exchanger model. Simulation results are discussed in Section 3. The conclusions are summarized in the final section.

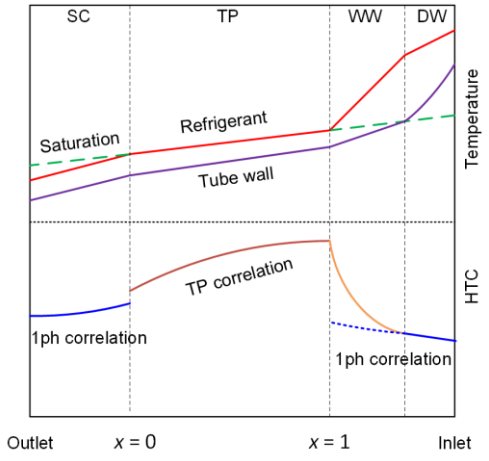

Fig.1 Flow regimes in a condenser

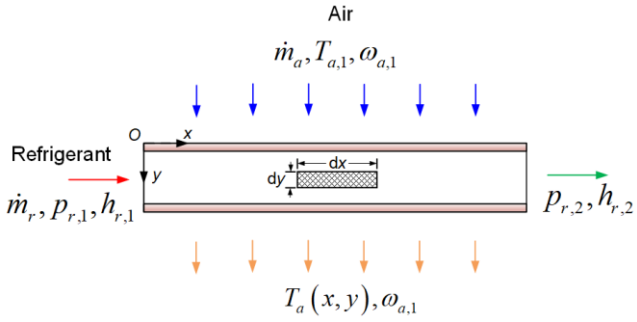

Fig. 2 Schematic of air-to-refrigerant cross-flow

2. MODEL DEVELOPMENT

The presented heat exchanger model is based on a tube-by-tube approach, i.e., the performance of each tube, associated with different refrigerant and air parameters, is evaluated separately. Simulation starts with the refrigerant inlet tube of a given circuit and progresses consecutively to the following tubes until the outlet is reached. The heat transfer process between air and refrigerant in a cross flow configuration with one tube is shown in Fig. 2. It is assumed that refrigerant temperature varies only in the *x* direction, while air and wall temperatures vary in both the *x* and *y* directions since the fins prevent mixing in a plane normal to the air flow. This paper only focuses on with the modeling of condenser heat exchangers, there will be no mass transfer on the air side. For an understanding of evaporator modeling, readers are referred to Qiao and Laughman (2016).

In Fig. 2, *x* and *y* are the dimensionless length along the refrigerant flow and air flow directions, respectively. Imposing the energy balance over the air and refrigerant streams across the differential area *dxdy* yields

$$\dot{m}_a c_{p,a} dT_a dx = -U_o \left(T_a - T_r\right) dS \tag{1}$$

$$\dot{m}_r dh_r dy = -\dot{m}_a c_{p,a} dT_a dx \tag{2}$$

where U_o is the overall heat transfer coefficient based on the total external surface area, $U_o = 1/ (R_a + R_m + \phi R_r)$. Symbol *R* represents the thermal resistance which can be calculated based on ARI Standard 410 (2001). ϕ is the ratio of total external coil surface area S_o to the total internal surface area S_i, S_o/S_i. $dS = S_o dxdy$.

Integrating Eq. (1) gives the two-dimensional air temperature distribution

$$T_a\left(x,y\right) = T_r\left(x\right) - \left[T_r\left(x\right) - T_a\left(x,0\right)\right]\exp\left(-NTU \cdot y\right) \tag{3}$$

where *NTU* is the number of transfer units defined as $NTU = U_o S_o / \left(\dot{m}_a c_{p,a}\right)$.

Accordingly, the two-dimensional internal tube surface temperature is

$$T_{wi}\left(x,y\right) = \phi R_r \left[T_a\left(x,y\right) - T_r\left(x\right)\right] / R_{tot} + T_r\left(x\right) \tag{4}$$

Evidently the internal tube surface temperature changes along the air flow direction. Therefore, an average internal tube surface temperature along the *y* direction is needed to determine the onset point of the wet-wall desuperheating, since the refrigerant flow is assumed to be one-dimensional flow and its dew point temperature only changes along the *x* direction. Integrating Eq. (4) along the *y* direction results in

$$\bar{T}_{wi}\left(x\right) = \int_0^1 T_{wi}\left(x,y\right) dy = T_r\left(x\right) + \frac{\phi R_r}{R_{tot}} \frac{\exp\left(-NTU\right) - 1}{NTU} \left[T_r\left(x\right) - T_a\left(x,0\right)\right] \tag{5}$$

It is assumed that air inlet temperature is uniform along the tube length and given as an input, i.e., $T_a(x,0) = T_{a,1}$.

Integrating Eq. (2) along the *y* direction gives

$$\dot{m}_r dh_r \int_0^1 dy = -\dot{m}_a c_{p,a} dx \int_{T_a(x,0)}^{T_a(x,1)} dT_a \Rightarrow \dot{m}_r dh_r = -\dot{m}_a c_{p,a} \left[T_a\left(x,1\right) - T_{a,1}\right] dx \tag{6}$$

Neglecting the effect of pressure change on the specific enthalpy change and integrating Eq. (6) along the *x* direction gives the single-phase refrigerant temperature distribution

$$T_r\left(x\right) = T_{a,1} + \left(T_{r,1} - T_{a,1}\right)\exp\left(-C_r \gamma x\right) \tag{7}$$

where γ = 1- exp (-*NTU*), and C_r is the ratio of air capacitance to refrigerant capacitance, i.e., $C_r = \dot{m}_a c_{p,a} / \left(\dot{m}_r c_{p,r}\right)$

Substituting Eq. (7) into Eq. (5) and rearrangements yield

$$\bar{T}_{wi}\left(x\right) = T_{a,1} + \left(T_{r,1} - T_{a,1}\right)\left(1 - \frac{\gamma}{NTU}\frac{\phi R_r}{R_{tot}}\right)\exp\left(-C_r \gamma x\right) \tag{8}$$

Eq. (8) gives the formula of calculating the average tube wall surface temperature along the *x* direction, and it will be used to determine the transition point from dry-wall to wet-wall desuperheating. To ensure a continuous calculation of tube wall temperature, the local HTC instead of average HTC should be always used. However, for the calculation of refrigerant temperature, an average HTC between the inlet and the location *x* should be used since the HTC changes along the tube length.

The difference between the tube wall temperature and refrigerant dew point at location *x* is given as

$$\Delta T\left(x\right) = \bar{T}_{wi}\left(x\right) - T_{dew}\left(x\right) = T_{a,1} - T_{dew,1} + \left(T_{r,1} - T_{a,1}\right)\left(1 - \frac{\gamma}{NTU}\frac{\phi R_r}{R_{tot}}\right)\exp\left(-C_r \gamma x\right) + \left[T_{dew,1} - T_{dew}\left(x\right)\right] \tag{9}$$

where $T_{dew,1}$ is the refrigerant dew point at the inlet of the tube/segment.

Let $A=\left(T_{r,1}-T_{a,1}\right)\left(1-\frac{\gamma}{NTU}\frac{\phi R_r}{R_t}\right), B=C_r\gamma, C\left(x\right)=T_{dew,1}-T_{dew}\left(x\right), D=T_{a,1}-T_{dew,1}$, Eq. (9) can be rewritten as

$$\Delta T\left(x\right)=A\exp\left(-Bx\right)+C\left(x\right)+D \tag{10}$$

Obviously $A > 0$, $B > 0$, $C(x) > 0$ and $D < 0$. Differentiating Eq. (10) with respect to x yields

$$\frac{d\Delta T\left(x\right)}{dx}=-AB\exp\left(-Bx\right)+\frac{dC\left(x\right)}{dx} \tag{11}$$

where $dC(x)/dx$ is always positive. Applying the Clausius-Clapeyron relation, one can obtain

$$\frac{dC\left(x\right)}{dx}=-\frac{dT_{dew}\left(x\right)}{dx}=-\frac{dT_{dew}}{dp}\frac{dp_r\left(x\right)}{dx}=-\frac{T_{dew}\left(v_g-v_f\right)}{\Delta h_{fg}}\frac{dp_r\left(x\right)}{dx} \tag{12}$$

The pressure drop across the tube length from the inlet to the location x consists of frictional pressure drop and momentum pressure drop.

$$p_r\left(x\right)=p_{r,1}-\Delta p_{frict}-\Delta p_{mom}=p_{r,1}-\bar{\xi}Lx-G_r^2\left[v_r\left(x\right)-v_{r,1}\right] \tag{13}$$

where $\bar{\xi}$ is the average frictional pressure drop gradient $\bar{\xi}=\left[\xi\left(0\right)+\xi\left(x\right)\right]/2$, which can be evaluated using any single-phase frictional pressure drop correlations.

Differentiating Eq. (13) yields the derivative of refrigerant pressure with respect to the dimensionless length x

$$\frac{dp_r\left(x\right)}{dx}=-\bar{\xi}L-G_r^2\frac{dv_r\left(x\right)}{dx}=-\bar{\xi}L-G_r^2\left[\frac{\partial v_r}{\partial p_r}\frac{dp_r\left(x\right)}{dx}+\frac{\partial v_r}{\partial T_r}\frac{dT_r\left(x\right)}{dx}\right] \tag{14}$$

Rearranging Eq. (14) gives

$$\frac{dp_r\left(x\right)}{dx}=-\left(\bar{\xi}L+G_r^2\frac{\partial v_r}{\partial T_r}\frac{dT_r}{dx}\right)/\left(1+G_r^2\frac{\partial v_r}{\partial p_r}\right) \tag{15}$$

Differentiating Eq. (7) yields the derivative of refrigerant temperature with respect to x

$$\frac{dT_r\left(x\right)}{dx}=-C_r\gamma\left(T_{r,1}-T_{a,1}\right)\exp\left(-C_r\gamma x\right) \tag{16}$$

Substituting Eqs. (15) and (16) into Eq. (12) results in

$$\frac{dC\left(x\right)}{dx}=T_{dew}\left(v_g-v_f\right)\left[\bar{\xi}L-G_r^2\frac{\partial v_r}{\partial T_r}C_r\gamma\left(T_{r,1}-T_{a,1}\right)\exp\left(-C_r\gamma x\right)\right]/\left[\Delta h_{fg}\left(1+G_r^2\frac{\partial v_r}{\partial p_r}\right)\right] \tag{17}$$

where all the thermal properties are evaluated using the refrigerant state at x.

It is not difficult to note that $d\Delta T/dx$ is a monotonically increasing function of x, and the following relation holds

$$\frac{d\Delta T\left(x\right)}{dx}\in\left(-\infty,\frac{dC\left(x\right)}{dx}+\varepsilon\right)\text{ for }x\in\left(-\infty,+\infty\right) \tag{18}$$

where ε is a sufficiently small number.

Eq. (18) indicates that there is always one solution that satisfies $d\Delta T/dx = 0$. Let $x_{\min}$ be this solution, which can be solved numerically using Newton's method, one can then have

$$\frac{d\Delta T\left(x\right)}{dx}=\begin{cases}<0, & if\ x<x_{\min}\\ 0, & if\ x=x_{\min}\\ >0, & if\ x>x_{\min}\end{cases} \tag{19}$$

From the knowledge of calculus, $x = x_{\min}$ is a minimum point of $\Delta T(x)$. Meanwhile, $\Delta T(x)$ decreases monotonically when $x < x_{\min}$, and increases monotonically when $x > x_{\min}$.

If $\Delta T(x = 0) \le 0$, it indicates that the internal tube wall temperature is equal or lower than the dew point of refrigerant vapor at the inlet of the current calculation domain (tube or segment). Therefore, refrigerant enters the tube/segment with wet-wall desuperheating and there is no dry-wall desuperheating in this tube/segment.

If $\Delta T(x = 0) > 0$, it indicates that the internal tube wall temperature is greater than the dew point of refrigerant vapor at the inlet of the current calculation domain. Therefore, refrigerant enters the tube/segment with dry-wall desuperheating. Then it needs to determine whether or not transition from dry-wall to wet-wall desuperheating occurs in the current tube/segment. There are overall 7 different cases.

Case 1: If $x_{\min} \le 0$, then the current tube/segment is entirely dry-wall desuperheating.

As discussed previously, $\Delta T(x)$ is a monotonically increasing function of x when $x > x_{min}$. Therefore $\Delta T\left(x \middle| x \in (0,1]\right) > \Delta T\left(x = 0\right) > 0$, meaning that the temperature difference between the tube wall and refrigerant dew point increases along the tube length and is always greater than zero. Obviously, the entire tube/segment will be in dry-wall desuperheating, and the tube wall refrigerant profile will never intersect with refrigerant dew point in this tube/segment. In this case, the function $\Delta T(x)$ is graphically represented in Fig. 3a and 3b, and the corresponding temperature profiles of the tube wall and refrigerant dew point is given in Fig. 4a.

Case 2: If $x_{min} \geq 1 \& \Delta T\left(x = 1\right) > 0$, then the entire tube/segment is dry-wall desuperheating.

Since $\Delta T(x)$ is a monotonically decreasing function of x when $x < x_{min}$, $\Delta T\left(x \middle| x \in [0,1)\right) > \Delta T\left(x = 1\right) > 0$. The temperature difference between the internal tube wall and refrigerant dew point decreases along the tube length and is always greater than zero. The internal tube wall temperature profile will never intersect with refrigerant dew point temperature in this tube/segment. In this case, the function $\Delta T(x)$ is graphically represented in Fig. 3c, 3d and 3e, and the corresponding temperature profiles of the tube wall and refrigerant dew point is given in Fig. 4b.

Case 3: If $x_{min} \geq 1 \& \Delta T\left(x = 1\right) = 0$, then the entire tube/segment is dry-wall desuperheating.

The internal tube wall temperature profile will intersect with refrigerant dew point at the end of this tube/segment, meaning that the inlet of the next tube/segment will be the onset point of wet-wall desuperheating. In this case, the function $\Delta T(x)$ is graphically represented in Fig. 3f, and the corresponding temperature profiles of the tube wall and refrigerant dew point is given in Fig. 4c.

Case 4: If $x_{min} \geq 1 \& \Delta T\left(x = 1\right) < 0$, transition from dry-wall to the wet-wall desuperheating occurs in this tube/segment.

It is evidently that $\Delta T\left(x = 0\right) > 0 > \Delta T\left(x = 1\right)$ in this case. Since $\Delta T(x)$ is a continuous function of x, there must be a solution in the interval [0, 1] that satisfies $\Delta T(x) = 0$, meaning that only a portion of the tube/segment is dry-wall desuperheating and transition from dry-wall to wet-wall occurs in this tube/segment. In this case, the function $\Delta T(x)$ is graphically represented in Fig. 3g, and the corresponding temperature profiles of the tube wall and refrigerant dew point is given in Fig. 4d.

Case 5: If $0 < x_{min} < 1 \& \Delta T\left(x = x_{min}\right) > 0$, then the entire tube/segment is dry-wall desuperheating.

The temperature difference between the tube wall and refrigerant dew point decreases first, reaches the minimum at $x = x_{min}$, and increases thereafter. Since the minimum temperature difference is greater than zero, one can have $\Delta T\left(x \middle| x \in [0, x_{min}) \cup (x_{min,}, 1]\right) > \Delta T\left(x = x_{min}\right) > 0$, meaning that the tube wall temperature profile will never intersect with refrigerant dew point. In this case, the function $\Delta T(x)$ is graphically represented in Fig. 3h, and the corresponding temperature profiles of the tube wall and refrigerant dew point is given in Fig. 4e.

Case 6: If $0 < x_{min} < 1 \& \Delta T\left(x = x_{min}\right) = 0$, transition from dry-wall to wet-wall desuperheating occurs at $x = x_{min}$.

The temperature profile of the internal tube wall is tangent to refrigerant dew point temperature profile at $x = x_{min}$. Therefore, only a portion of the tube/segment is dry-wall desuperheating. In this case, the function $\Delta T(x)$ is graphically represented in Fig. 3i, and the corresponding temperature profiles of the tube wall and refrigerant dew point is given in Fig. 4f.

Case 7: If $0 < x_{min} < 1 \& \Delta T\left(x = x_{min}\right) < 0$, transition from dry-wall to wet-wall desuperheating occurs in this tube/segment.

The temperature profile of the internal tube wall will intersect with refrigerant dew point temperature profile twice. Based on the location of intersection points, there are three possibilities.

(i) If $\Delta T(x = 1) > 0$, both intersection points are in this tube/segment. The first intersection point lies in the interval (0, x_{min}), and the second intersection lies in the interval (x_{min}, 1), In this case, the function $\Delta T(x)$ is graphically represented in Fig. 3j, and the corresponding temperature profiles of the tube wall and refrigerant dew point is given in Fig. 4g.

(ii) If $\Delta T(x = 1) < 0$, only one intersection point is in this tube/segment and the other intersection point is outside this tube/segment. In this case, the function $\Delta T(x)$ is graphically represented in Fig. 3k, and the corresponding temperature profiles of the tube wall and refrigerant dew point is given in Fig. 4h.

(iii) If $\Delta T(x = 1) = 0$, the first intersection point is inside this tube/segment and the other intersection point is right at the outlet of the tube/segment. In this case, the function $\Delta T(x)$ is graphically represented in Fig. 3l, and the corresponding temperature profiles of the tube wall and refrigerant dew point is given in Fig. 4i.

For all these three possibilities, only the first intersection point is the true onset point of wet-wall desuperheating. Therefore, this onset point should be always iterated within the interval (0, x_{min}) such that $\Delta T = 0$ to ensure the correct solution.

2.1 Dry-wall Desuperheating

Using the method described previously to determine whether or not the entire tube/segment is dry-wall desuperheating. If yes, refrigerant outlet temperature can be computed using Eq. (7) with $x = 1$. Refrigerant outlet enthalpy $h_{r,2}$ can be computed using the property routines given $p_{r,2}$ and $T_{r,2}$.

$$T_{r,2} = T_{a,1} + \left(T_{r,1} - T_{a,1}\right)\exp\left(-C_r\gamma\right) \tag{20}$$

The average temperature of air stream leaving the tube/segment can be obtained as

$$\bar{T}_{a,2} = \int_{x=0}^{x=1} T_a\left(x,1\right)dx = \dot{m}_r\left(h_{r,2} - h_{r,1}\right)/\left(\dot{m}_a c_{p,a}\right) + T_{a,1} \tag{21}$$

If transition from dry-wall to wet-wall desuperheating occurs in the tube/segment, the fraction of dry-wall desuperheating needs to be iterated such that the temperature of the internal tube wall is equal to refrigerant dew point at the transition point. Then the refrigerant state leaving the dry-wall portion can be calculated similarly and will be used as the inlet state of the remaining portion of the tube length, which will be wet-wall desuperheating.

It is worthwhile to point out that both refrigerant HTC and frictional DP gradient change along the tube length. To ensure the best prediction accuracy, therefore, the arithmetic mean of the HTC and frictional DP gradient between the inlet and the outlet should be used.

2.2 *Wet-wall Desuperheating*

Both sensible and latent heat transfer occurs during wet-wall desuperheating. Sensible heat transfer occurs between the bulk superheated refrigerant and the liquid film surface, and its driving force is the difference between the bulk temperature and refrigerant dew point. Latent heat transfer occurs when saturated refrigerant vapor condenses, and its driving force is the difference between refrigerant dew point and tube wall temperature. Therefore, the HTC during wet-wall desuperheating can be expressed as the combination of single-phase and two-phase correlations (Kondou and Hrnjak, 2012)

$$\alpha_{wet} = \left[\alpha_{sh}\left(T_r - T_{dew}\right) + \alpha_{tp}\left(T_{dew} - T_{wi}\right)\right]/\left(T_r - T_{wi}\right) \tag{22}$$

where T_r is the bulk refrigerant temperature.

Meanwhile, the frictional pressure drop gradient can be determined similarly

$$\xi_{wet} = \left[\xi_{sh}\left(T_r - T_{dew}\right) + \xi_{tp}\left(T_{dew} - T_{wi}\right)\right]/\left(T_r - T_{wi}\right) \tag{23}$$

Since the overall heat transfer temperature difference during wet-wall desuperheating is defined as the same as that in dry-wall desuperheating, as indicated as Eq. (22), all the equations for dry-wall desuperheating are applicable for wet-wall except that the HTC and DP need to be calculated differently and iteration of the tube wall temperature is involved.

Similarly, if transition from wet-wall desuperheating to two-phase condensation occurs in the tube/segment, the fraction of wet-wall desuperheating needs to be iterated such that the bulk refrigerant quality is equal to 1. Then the refrigerant bulk state leaving the wet-wall portion is the saturated vapor and will be used as the inlet state of the remaining portion of the tube, which will be the two-phase condensation regime.

2.3 *Two-phase Condensation*

In two-phase, refrigerant temperature is dependent upon both pressure and quality. To avoid complex computation involving numerical integration, it is assumed that refrigerant temperature varies linearly along the tube length, i.e.

$$T_r\left(x\right) = T_{r,1} + \int_0^x \frac{dT_r}{dz}dz \approx T_{r,1} + \left(T_{r,2} - T_{r,1}\right)x \tag{24}$$

Substituting Eq. (24) into Eq. (1) and integrating results in the heat rejection across the tube

$$Q = \dot{m}_a c_{p,a}\gamma\int_{x=0}^{x=1}\left[\left(T_{r,1} + \int_0^x \frac{dT_r}{dz}dz\right) - T_{a,1}\right]dx \approx \dot{m}_a c_{p,a}\gamma\left[\left(T_{r,1} + T_{r,2}\right)/2 - T_{a,1}\right] \tag{25}$$

The specific enthalpy of refrigerant leaving the tube can be iteratively computed since refrigerant outlet temperature $T_{r,2} = T(p_2, h_2)$ is based on the energy balance $Q = \dot{m}_r\left(h_{r,1} - h_{r,2}\right)$.

Similarly, if transition from two-phase condensation to the subcooled regime occurs in the tube/segment, the fraction of the two-phase regime needs to be iterated such that the refrigerant quality is equal to 0. Then the refrigerant state

leaving the two-phase portion is the saturated liquid and will be used as the inlet state of the remaining portion of the tube, which will be the subcooled regime.

2.4 *Subcooled*

The subcooled regime is the last flow regime in the condenser, and all the equations for dry-wall desuperheating are applicable for this regime. Since the single-phase and two-phase HTC correlations generally are not continuous at x = 0, the HTC within the interval $x \in [0, 0.02]$ is linearly interpolated to avoid numerical failures.

2.5 Model Algorithm

Outside the module of tube-by-tube analysis, there are three higher level nested iteration loops. The innermost iteration loop is to compute refrigerant flow distribution for all the circuitries. The next iteration loop uses the successive substitution approach to compute the air temperature entering each tube. The outermost iteration loop is to compute the air flow distribution for all the face tubes. The innermost and outermost iteration loops involve solving a large-scale system of non-linear pressure drop equalization equations. In order to reduce the computational cost, these non-linear pressure drop equalization equations are linearized and solved by a method which is similar to the approach used to solve air flow redistribution due to non-uniform frost growth (Qiao *et al.*, 2017).

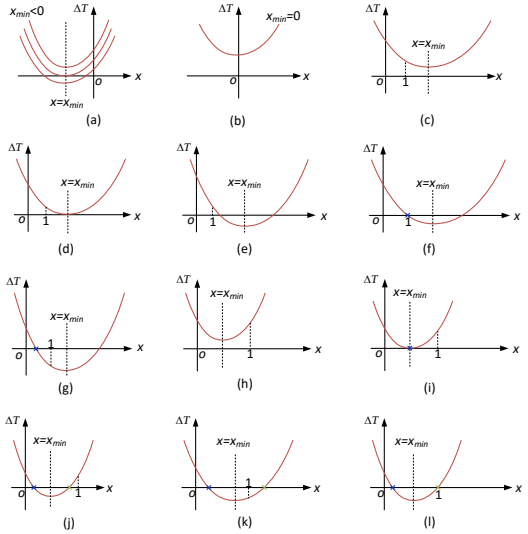

Fig. 3 Possible profiles of $\Delta T(x)$ for dry-wall desuperheating

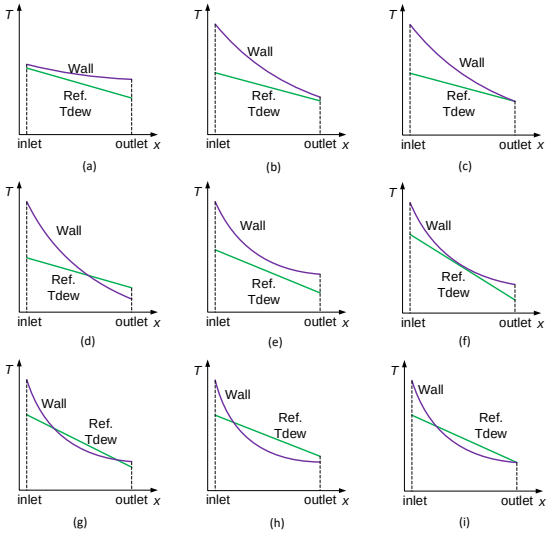

Fig. 4 Possible temperature profiles of T_{wi} and T_{dew} for dry-wall desuperheating

3. RESULTS AND DISCUSSIONS

The proposed heat exchanger model has been developed in the C# programming environment. All the refrigerant properties are evaluated based on the REFPROP 9.0 database (Lemmon *et al.*, 2010). Correlations are used to calculate the heat transfer coefficients and the pressure drops on both refrigerant side and air side are given in Table 1.

To verify the existence of wet-wall desuperheating in a condenser with refrigerant vapor entering at the inlet, simulation studies are conducted. The geometry and operating conditions of the simulated coil are given in Table 2. The fraction of the heat exchanger that each flow regime accounts for under different inlet superheats is plotted in Fig. 5. Based on the simulation results, it can be readily observed that wet-wall desuperheating always exists as long as refrigerant vapor enters the condenser. However, dry-wall desuperheating does not occur until the inlet superheat reaches 25 K. Meanwhile, it can be shown that dry-wall desuperheating always occurs near the inlet of the condenser and its length increases as refrigerant inlet temperature increases. The profiles of refrigerant temperature, tube wall temperature and refrigerant saturation temperature are illustrated in Fig. 6 for the case with the inlet superheat of 35 K. For this case, the tube wall temperature is much higher than refrigerant dew point at the inlet of the condenser, and therefore the refrigerant vapor starts to lose its superheat by dry-wall desuperheating. As the tube wall temperature drops below refrigerant dew point near the end of the 1st tube, wet-wall desuperheating occurs and continues in the 2nd tube. A large portion of the coil is in the two-phase condensation regime (from the 3rd tube to a portion of the last tube), and the refrigerant leaves the coil with subcooling of around 5 K.

The above results clearly show that neglecting wet-wall desuperheating could lead to substantial errors in the performance prediction of heat exchangers. To quantify these errors, a group of simulations are performed to compare the predicted heat loads between with and without taking into account wet-wall desuperheating. Using the same heat exchanger described in Table 2, refrigerant mass flow rate varies from 0.008 kg/s to 0.3 kg/s, refrigerate inlet saturation temperature varies from 40 °C to 55 °C, and refrigerant inlet superheat varies from 5 K to 60 K. The comparison of heat load between with and without wet-wall desuperheating is shown in Fig. 7. It can be noted that neglecting the wet-wall phenomenon generally results in under prediction of heat exchanger performance. Especially when the refrigerant leaves the condenser in a two-phase state, the prediction errors can be as large as 10%. When refrigerant leaves the condenser with a large amount of subcooling, the prediction errors are typically within 2-3%. Interestingly, when the flow configuration changes from counter-flow to parallel-flow, neglecting wet-wall desuperheating may lead to slight over prediction of heat load for the cases with a very long subcooled zone. In these cases, refrigerant in the tubes at the end of refrigerant circuitry might gain heat from the air stream instead of losing heat, if the air temperatures leaving the preceding tube banks are high enough. In the parallel-flow configuration, accounting for wet-wall desuperheating results in a shrunk desuperheating zone and a prolonged two-phase zone in the first tube bank. Therefore, air temperature leaving the first tube bank will be higher compared to the cases that neglect wet-wall desuperheating. With higher air temperatures leaving the first tube bank, the subcooled refrigerant in the tubes close to the end of the condenser will gain more heat from the air stream, resulting in smaller heat load, as shown in Fig. 8.

Table 1 Correlation summary

Air side	
Heat transfer	Wang *et al.* (1999)
Pressure drop	Wang *et al.* (1999)
Single-phase	
Heat transfer	Gnielinski (1976)
Pressure drop	Blasius (Incropera *et al.*, 2007)
Wet-wall Desuperheating	
Heat transfer	Kondou-Hrnjak (2012)
Pressure drop	Linear combination of Blasius and Friedel
Condensation	
Heat transfer	Cavallini (2006)
Pressure drop	Friedel (1979)

Table 2 Coil geometry

Parameter	**Unit**	**Value**
Tube length	mm	1000
Tube outer diameter	mm	7.9
Tube wall thickness	mm	0.8
Tubes per row	-	18
Number of rows	-	2
Number of circuits	-	3
Tube horizontal spacing	mm	17.7
Tube vertical spacing	mm	20.4
Fins per inch	-	15.8
Fin thickness	mm	0.1
Fin type	-	Louver fin
Flow configuration	-	Counter flow
Operating Conditions		
Refrigerant type	-	R32
Refrigerant mass flow rate	kg/s	0.022
Refrigerant inlet saturation temperature	°C	50
Refrigerant inlet superheat	K	0.5 - 60
Air volumetric flow rate	m^3/s	0.5
Air inlet temperature	°C	35

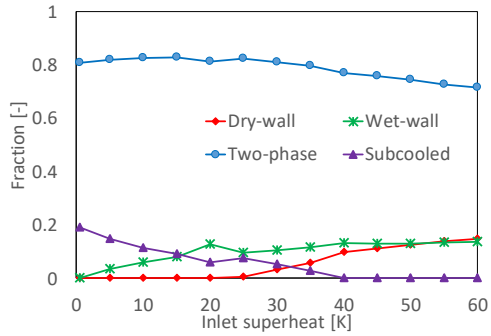

Fig. 5 Breakdown of each flow regime under different superheat

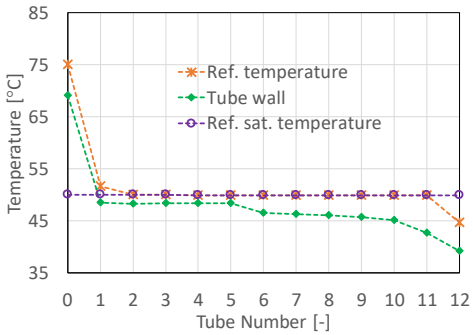

Fig. 6 Temperature profiles of refrigerant, tube wall and refrigerant saturation

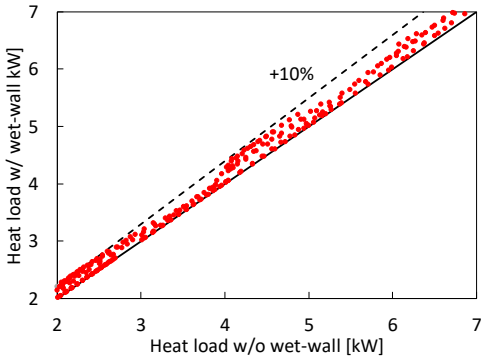

Fig. 7 Heat load comparison (counter-flow)

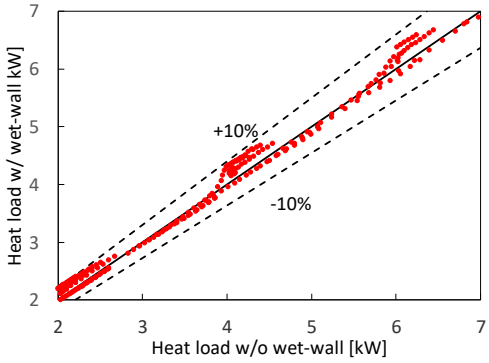

Fig. 8 Heat load comparison (parallel-flow)

4. CONCLUSIONS

A new air-cooled fin-and-tube condenser heat exchanger model has been developed to take into account the wet-wall desuperheating phenomenon. Rigorous algorithms have been developed to capture the boundary between different flow regimes. Each flow regime is analyzed separately and their respective lengths are iterated to eliminate numerical discontinuities. Particularly, the determination of the existence of dry-wall desuperheating is handled with extreme care to ensure correct calculation of heat transfer. Meanwhile, the refrigerant side is modeled to handle any boundary conditions, and the techniques can be easily extended to other types of heat exchangers, e.g., water-cooled heat exchangers or microchannel heat exchangers. A tube-by-tube analysis (which can be easily extended to a segment-by-segment analysis) is adopted to allow for the simulation of complex tube circuitries. Simulation studies show that wet-wall desuperheating always exists in the condenser with refrigerant vapor entering at the inlet, whereas dry-wall desuperheating might not exist at all for the cases with low inlet superheat. Meanwhile, it is found that neglecting wet-wall desuperheating can lead to significant prediction errors for heat load, which can be as large as 10% under some conditions.

NOMENCLATURE

Symbols		***Subscripts***	
c_p	specific heat	a	air
C_r	capacitance ratio	dew	dew point
G	mass flux	f	saturated liquid
h	specific enthalpy	fg	liquid to vapor
L	tube length	frict	friction
$\dot{m}$	mass flow rate	g	saturated vapor
NTU	number of transfer units	m	metal

p	pressure	mom	momentum
Q	heat transfer rate	o	external
R	thermal resistance	r	refrigerant
S	surface area	sh	superheated
T	temperature	tot	total
U	overall heat transfer coefficient	tp	two-phase
v	specific volume	wet	wet-wall
ϕ	surface area ratio	wi	internal tube wall
α	heat transfer coefficient		
ξ	frictional DP gradient		
Δ	difference		

REFERENCES

ARI Standard 410, 2001. Forced-circulation air-cooling and air-heating coils.

Cavallini, A., Del Col D., Doretti, L., Matkovic, M., Rossetto, L., Zilio, C., Censi, G., 2006. Condensation in horizontal smooth tubes: a new heat transfer model for heat exchanger design. *Heat Transfer Eng.* 27 (8), 31-38.

Domanski, P., and Didion. D., 1983. Computer modeling of the vapor compression cycle with constant flow area expansion device. *Building Science Series* 155.

Friedel, L., 1979. Improved friction pressure drop correlation for horizontal and vertical two phase pipe flow. Proc. European Two-Phase Flow Group Meeting, Ispra, Italy, Paper No. E2.

Gnielinksi, V., 1976. New equation of heat and mass transfer in turbulent pipe and channel flow. *Int. Chem. Eng.* 16, 359-367.

Incropera, F.P., Dewitt, D.P., Bergman, T.L., Lavine, A.S., 2007. Fundamentals of heat and mass transfer (6th ed). John Wiley & Sons Inc., New Jersey, USA.

Jiang, H., Aute. V., Radermacher, R., 2006. CoilDesigner: a general purpose simulation and design tool for air-to-refrigerant heat exchangers. *Int. J. Refrigeration* 29, 601-610.

Kondou, C. and Hrnjak, P., 2012. Condensation from superheated vapor flow of R744 and R410A at supercritical pressures in a horizontal smooth tube. *Int. J. Heat Mass Transfer* 55, 2779-2791.

Lee, J. and Domanski, P.A., 1997. Impact of air and refrigerant maldistributions on the performance of finned-tube evaporators with R-22 and R-407C. Report DOE/CE/23810-81 for ARI, National Institute of Standards and Technology, Gaithersburg, MD.

Lemmon, E.W., Huber, M.L., McLinden, M.O., 2010. NIST Reference Fluid Thermodynamic and Transport Properties - REFPROP Version 9.0. National Institute of Standard and Technology.

Liang, S.Y., Wong, T.N., Nathan, G.K., 2001. Numerical and experimental studies of refrigerant circuitry of evaporator coils. *Int. J. Refrigeration* 24, 823 - 833.

Liu, J., Wei, W., Ding, G., Zhang, C., Fukaya, M., Wang, K. and Inagaki, T., 2004. A general steady state mathematical model for fin-and-tube heat exchanger based on graph theory. *Int. J. Refrigeration* 27 (8), 965-973.

Meyer, M. and Hrnjak, P., 2014. Pressure drop in condensing superheated zone. 15th International Refrigeration and Air Conditioning Conference at Purdue, West Lafayette, IN.

Meyer, M. and Hrnjak, P., 2017. Flow regimes during condensation in superheated zone. *Int. J. Refrigeration* 84, 336-343.

Qiao, H., Aute, V., Radermacher, R., 2017. Dynamic modeling and characteristic analysis of a two-stage vapor injection heat pump system under frosting conditions. *Int. J. Refrigeration* 84, 181-197.

Qiao, H. and Laughman, C., 2016. Modeling of finned-tube heat exchangers: a novel approach to the analysis of heat and mass transfer under cooling and dehumidifying conditions. 16th International Refrigeration and Air Conditioning Conference at Purdue, West Lafayette, IN.

Thome, J.R., 2004. Engineering Data Book III. Wolverine Tube Inc.

Wang, C.C., Chi, K.Y., Chang, C.J., 2000. Heat transfer and friction characteristics of plain fin-and-tube heat exchangers, part II: Correlation. *Int. J. Heat Mass Transfer* 43, 2693-2700.